Thermosensitive, Soft Glassy and Structural Colored Colloidal Array in Ionic Liquid: Colloidal Glass to Gel Transition

ARTICLE *in* LANGMUIR · OCTOBER 2010

Impact Factor: 4.46 · DOI: 10.1021/la103716q · Source: PubMed

5 AUTHORS, INCLUDING:

Kazuhide Ueno
Yamaguchi University
69 PUBLICATIONS **1,245** CITATIONS
SEE PROFILE

Takeshi Ueki
National Institute for Materials Science
48 PUBLICATIONS **1,171** CITATIONS
SEE PROFILE

Masayoshi Watanabe
Yokohama National University
350 PUBLICATIONS **14,354** CITATIONS
SEE PROFILE

Langmuir
Article
pubs.acs.org/Langmuir

Thermosensitive, Soft Glassy and Structural Colored Colloidal Array in Ionic Liquid: Colloidal Glass to Gel Transition

Kazuhide Ueno,[†] Aya Inaba,[†] Takeshi Ueki,[†] Masashi Kondoh,[‡] and Masayoshi Watanabe*[,†]

[†]*Department of Chemistry and Biotechnology and* [‡]*Instrumental Analysis Center, Yokohama National University, 79-5 Tokiwadai, Hodogaya-ku, Yokohama 240-8501, Japan*

Received September 16, 2010. Revised Manuscript Received October 3, 2010

A novel soft material comprising thermosensitive poly(benzyl methacrylate)-grafted silica nanoparticles (PBnMA-*g*-NPs) and the ionic liquid (IL), 1-ethyl-3-methylimidazolium bis(trifluoromethane sulfonyl)amide ($[C_2mim][NTf_2]$), was fabricated. The thermosensitive properties were studied over a wide range of particle concentrations and temperatures. PBnMA-*g*-NPs in the IL underwent the lower critical solution temperature (LCST) phase transition at lower temperatures with a broader transition temperature range as compared to the free PBnMA solution. Highly concentrated suspensions formed soft glassy colloidal arrays (SGCAs) exhibiting a soft-solid behavior and angle-independent structural color. For the first time, we report a discrete change in the angle-independent structural color of SGCAs with temperature because of a temperature-induced colloidal glass-to-gel transition. The interparticle interaction changed from repulsive to attractive at the LCST temperature, and it was characterized by a V-shaped rheological response and a direct electron microscope observation of the colloidal suspension in the IL. With unique rheological and optical properties as well as properties derived from the IL itself, the thermosensitive SGCAs may be of interest as a new material for a wide range of applications such as electrochemical devices and color displays.

Introduction

There has been a growing interest in composite materials comprising ionic liquids (ILs) and polymers and/or colloids, particularly for their application in solid electrolytes,[1−3] separation membranes,[4,5] catalyst supports,[6] and electroactive soft actuators.[7,8] This upsurge in the interest mainly arises from the remarkable physicochemical properties of ILs, such as negligible volatility, thermal stability, nonflammability, and high ionic conductivity. A number of composite soft materials containing ILs have been successfully prepared by employing different additives such as carbon nanotubes,[9] compatible polymer networks,[10−12] crystalline polymers,[13,14] inorganic silica networks,[15] silica nanoprticles,[16,17] and block copolymers.[18] However, the additive components do not always act only as mechanical supports for the ILs. The introduction of a novel functionality into the additive components of IL-based composites would be of great interest because this fascinating class of functional soft materials may be promising for use in special working conditions (e.g., under vacuum and high temperature). In this study, we demonstrate an interesting change in the optical and rheological properties of a novel functional colloidal array consisting of an IL and thermosensitive particles.

As stimuli-responsive polymers have been widely used to fabricate functional soft materials in aqueous and organic media,[19−21] their use is a feasible approach to develop functional soft materials based on ILs. Recently, we reported that certain polymers exhibit stimuli-responsiveness in ILs.[22−25] Poly(*N*-isopropylacrylamide) (PNIPAm), which is the most well-studied thermoresponsive polymer showing the lower critical solution temperature (LCST) phase behavior in aqueous media, underwent the opposite upper critical solution temperature (UCST) phase behavior in an IL.[26] On the other hand, poly(benzyl methacrylate) (PBnMA) showed the

*To whom correspondence should be addressed. Fax: +81-45-339-3955. E-mail: mwatanab@ynu.ac.jp.

(1) Watanabe, M.; Yamada, S.; Sanui, K.; Ogata, N. *J. Chem. Soc., Chem. Commun.* **1993**, 929.
(2) Shin, J.-H.; Henderson, W. A.; Passerini, S. *Electrochem. Commun.* **2003**, *5*, 1016.
(3) Stathatos, E.; Lianos, P.; Zakeeruddin, S. M.; Liska, P.; Grätzel, M. *Chem. Mater.* **2003**, *15*, 1825.
(4) Tang, J. B.; Tang, H. D.; Sun, W. L.; Plancher, H.; Radosz, M.; Shen, Y. *Chem. Commun.* **2005**, 3325.
(5) Baltus, R. E.; Counce, R. M.; Culbertson, B. H.; Luo, H.; DePaoli, D. W.; Dai, S.; Duckworth, D. C. *Sep. Sci. Technol.* **2005**, *40*, 525.
(6) Carlin, R. T.; Fuller, J. *Chem. Commun.* **1997**, 1345.
(7) Fukushima, T.; Asaka, K.; Kosaka, A.; Aida, T. *Angew. Chem., Int. Ed.* **2005**, *44*, 2410.
(8) Saito, S.; Katoh, Y.; Kokubo, H.; Watanabe, M.; Maruo, S. *J. Miromech. Microeng.* **2009**, *19*, 035005.
(9) Fukushima, T.; Kosaka, A.; Ishimura, Y.; Yamamoto, T.; Takigawa, T.; Ishii, N.; Aida, T. *Science* **2003**, *300*, 2072.
(10) Noda, A.; Watanabe, M. *Electrochim. Acta* **2000**, *45*, 1265.
(11) Sneddon, P.; Cooper, A. I.; Scott, K.; Winterton, N. *Macromolecules* **2003**, *36*, 4549.
(12) Susan, M. A. B. H.; Kaneko, K.; Noda, A.; Watanabe, M. *J. Am. Chem. Soc.* **2005**, *127*, 4976.
(13) Carlin, R. T.; Delong, H. C.; Fuller, J.; Trulove, P. C. *J. Electrochem. Soc.* **1994**, *141*, L73.
(14) Kawaushi, T.; Kumaki, J.; Okoshi, K.; Yashima, E. *Macromolecules* **2005**, *38*, 9155.
(15) Néouze, M.-A.; Bideau, J. L.; Gaveau, P.; Bellayer, S.; Vioux, A. *Chem. Mater.* **2006**, *18*, 3931.
(16) Wang, P.; Zakeeruddin, S. M.; Comte, P.; Exnar, I.; Grätzel, M. *J. Am. Chem. Soc.* **2003**, *125*, 1166.
(17) Katakabe, T.; Kawano, R.; Watanabe, M. *Electrochem. Solid-State Lett.* **2007**, *10*, F23.
(18) He, Y.; Boswell, P. G.; Bühlmann, P.; Lodge, T. P. *J. Phys. Chem. B* **2007**, *111*, 4645.
(19) Osada, Y.; Gong, J. P. *Prog. Polym. Sci.* **1993**, *18*, 187.
(20) Hinze, L.; Uemasu, I.; Dai, F.; Braun, M. *Curr. Opin. Colloid Interface Sci.* **1996**, *1*, 502.
(21) Ahn, S.-K.; Kasi, R. M.; Kim, S.-C.; Sharma, N.; Zhou, Y. *Soft Matter* **2008**, *4*, 1151.
(22) Ueki, T.; Watanabe, M. *Macromolecules* **2008**, *41*, 3739.
(23) Tsuda, R.; Kodama, K.; Ueki, T.; Kokubo, H.; Imabayashi, S.; Watanabe, M. *Chem. Commun.* **2008**, 4939.
(24) Ueki, T.; Yamaguchi, A.; Ito, N.; Kodama, K.; Sakamoto, J.; Ueno, K.; Kokubo, H.; Watanabe, M. *Langmuir* **2009**, *25*, 8845.
(25) Ueki, T.; Ayusawa Arai, A.; Kodama, K.; Kaino, S.; Takata, N.; Morita, T.; Nishikawa, K.; Watanabe, M. *Pure Appl. Chem.* **2009**, *81*, 1829.
(26) Ueki, T.; Watanabe, M. *Chem. Lett.* **2006**, *35*, 964.

LCST phase separation in ILs at a discrete phase separation temperature (T_c).[27] Furthermore, systematic studies revealed that the T_c of PBnMA could be tuned by copolymerization with solvophobic styrene and solvophilic methyl methacrylate (MMA)[27,28] and by structural modification of PBnMA[29] as well as ionic structures of the IL solvent.[27] These systems were evolved to produce stimuli-responsive soft materials containing an IL, such as thermoresponsive ion gels that undergo reversible volume phase transition[26,27] and thermoresponsive micellization systems using diblock copolymers.[30,31] Lodge and co-workers have used thermosensitive multiblock copolymers to prepare a physical ion gel that exhibits a thermally reversible sol−gel transition.[32,33]

In this study, we focused on silica colloidal suspensions in ILs from fundamental and practical viewpoints. We previously reported the colloidal stability of dilute suspensions of unmodified and poly(methyl methacrylate) (PMMA)-grafted silica nanoparticles in ILs[34] and studied the properties of soft materials fabricated by colloidal self-assembly of the colloidal particles in ILs.[35−38] The unmodified silica nanoparticles were colloidally unstable and flocculate in the ILs, and they formed a particulate network. Thus, the system behaved as a gel (nanocomposite ion gel) with the addition of a small amount (a few wt %) of silica nanoparticles. The nanocomposite ion gels showed high ionic conductivity comparable to that of the pure IL and shear-induced gel−sol transitions.[35,36] The suspension of the sterically stabilized PMMA-grafted particles formed a soft glass in a high concentration regime and exhibited homogeneous, nonbrilliant, and angle-independent structural colors,[37,38] which are distinct from the optical properties of the well-studied structural-colored materials based on a colloidal crystalline array.[39−41] It was found that such unique optical properties were attributed to the short-range ordered structure of the soft glassy colloidal arrays (SGCAs) formed in the ILs.[37,38]

In this study, thermosensitive PBnMA-grafted silica nanoparticles (PBnMA-*g*-NPs) were synthesized via surface-initiated atom transfer radical polymerization (ATRP). First, we studied the temperature-responsive colloidal stability of a dilute suspension of PBnMA-*g*-NPs in ILs. The primary purpose here was to understand the LCST phase behavior of the end-tethered PBnMA brush on the silica surface by comparing it to free PBnMA chains in the ILs. Furthermore, the SGCA comprising highly concentrated PBnMA-*g*-NPs and an IL was prepared, and its temperature-dependent rheological and optical properties were investigated. We demonstrated a temperature-induced colloidal glass-to-gel transition due to a change in the interparticle interactions from repulsive to attractive at the LCST temperature. This phenomenon was characterized by a V-shaped rheological response and structural color changes.

Experimental Section

Materials. Monodispersed silica colloidal particles (KE-P10, 120 nm in diameter) were purchased from Nippon Shokubai Co., Ltd. MMA and benzyl methacrylate (BnMA) monomers were distilled under reduced pressure over CaH_2 prior to use. CuBr was purified according to a previously reported procedure.[42] Other chemical reagents were used as received. The ionic liquid used in this study, 1-ethyl-3-methylimidazolium bis(trifluoromethane sulfonyl)amide ([C_2mim][NTf_2]), was synthesized according to a previously reported procedure.[43]

Preparation of Polymer-Grafted Silica Nanoparticles. Polymer-grafted silica nanoparticles, PMMA-*g*-NPs and PBnMA-*g*-NPs, were synthesized by surface-initiated atom-transfer radical polymerization (ATRP).[34,44] An ATRP surface initiator, (3-(2-bromo-2-methyl)propionyloxy)propyldimethylethoxysilane (BIDS), was synthesized according to previous studies.[44] Dry dichloromethane (200 mL), allyl alcohol (5.0 mL, 0.074 mol), and triethylamine (10.5 mL, 0.075 mol) were added into a three-necked flask under a nitrogen atmosphere. The flask was then cooled in an ice bath, and 2-bromoisobutyryl bromide (10.0 mL, 0.105 mol) was added. The mixture was stirred for 1 h at 0 °C and then for another 15 h at room temperature. The product was washed with a 1 N HCl aqueous solution and with water four times. After the solvent was removed by an evaporator, the remaining brown oil was distilled under reduced pressure (10 mmHg) at 64 °C and 11.9 g (71%) of allyl-2-bromo-2-methylpropionate (ABMP) was obtained. ABMP (11.9 g, 0.0573 mol), Karstedt's catalyst solution (400 μL), and xylene (2.5 mL) were added into a three-necked flask under a nitrogen atmosphere. Dimethylethoxysilane (10.0 g, 0.096 mol) was added dropwise, and the reaction was monitored by ^{1}H NMR until ABMP was completely consumed. After the reaction was complete, excess dimethylethoxysilane and the solvent were removed under vacuum at an elevated temperature. The surface initiator, BIDS, was obtained in a 64.5% yield (11.5 g) after distillation at 100 °C/2 mmHg. Immobilization of BIDS on the silica particles was conducted by heating the THF solution under refluxing conditions for 18 h. The surface initiator-modified silica nanoparticles were isolated by centrifugation and redispersed in THF. The initiator-modified particles were purified by repeated dispersion and centrifugation with a large amount of THF to remove the excess unreacted surface initiator.

A typical polymerization procedure for PBnMA-*g*-NPs is described below. CuBr (36.5 mg, 0.254 mmol) and $CuBr_2$ (6.59 mg, 0.0295 mmol) were added to a two-necked flask and evacuated at 65 °C for several hours. Next, dry anisole (24.5 mL) and *N*,*N*,*N*′,*N*″,*N*″-pentamethyldiethylenetriamine (59.3 μL, 0.284 mmol) were added. The ATRP surface-initiator-modified silica nanoparticles (3.78 g) and a free initiator, ethyl α-bromoisobutyrate (10 μL, 0.0385 mmol), were dispersed in BnMA (24.5 mL, 145 mmol) by ultrasonication and added into the flask. After the mixture was deoxygenated by four freeze−pump−thaw cycles, the colloidal dispersion was stirred vigorously to obtain a homogeneous suspension. Polymerization was carried out at 75 °C and was terminated by quenching with dry ice/methanol. The suspension was purified by reprecipitation using THF and 2-propanol with a small amount of HCl aqueous solution. The PBnMA-*g*-NPs were isolated from the mixture of free PBnMA and PBnMA-*g*-NPs by repeated centrifugation and redispersion in THF. The isolated PBnMA-*g*-NPs were reprecipitated again and finally dried for 24 h at 75 °C under vacuum. PMMA-*g*-NPs were also prepared by a similar procedure. The number-average molecular

(27) Ueki, T.; Watanabe, M. *Langmuir* **2007**, *23*, 988.
(28) Ueki, T.; Karino, T.; Kobayashi, Y.; Shibayama, M.; Watanabe, M. *J. Phys. Chem. B* **2007**, *111*, 4750.
(29) Kodama, K.; Nanashima, H.; Ueki, T.; Kokubo, H.; Watanabe, M. *Langmuir* **2009**, *25*, 3820.
(30) Ueki, T.; Watanabe, M.; Lodge., T. P. *Macromolecules* **2009**, *42*, 1315.
(31) Tamura, S.; Ueki, T.; Ueno, K.; Kodama, K.; Watanabe, M. *Macromolecules* **2009**, *42*, 6239.
(32) He, Y.; Lodge, T. P. *Chem. Commun.* **2007**, 2732.
(33) He, Y.; Lodge, T. P. *Macromolecules* **2008**, *41*, 167.
(34) Ueno, K.; Inaba, A.; Kondoh, M.; Watanabe, M. *Langmuir* **2008**, *24*, 5253.
(35) Ueno, K.; Hata, K.; Katakabe, T.; Kondoh, M.; Watanabe, M. *J. Phys. Chem. B* **2008**, *112*, 9013.
(36) Ueno, K.; Imaizumi, S.; Hata, K.; Watanabe, M. *Langmuir* **2009**, *25*, 825.
(37) Ueno, K.; Inaba, A.; Sano, Y.; Kondoh, M.; Watanabe, M. *Chem. Commun.* **2009**, 3603.
(38) Ueno, K.; Sano, Y.; Inaba, A.; Kondoh, M.; Watanabe, M. *J. Phys. Chem. B* **2010**, *114*, 13095.
(39) Holtz, J. H.; Asher, S. A. *Nature* **1997**, *389*, 829.
(40) Arsenault, A. C.; Puzzo, D. P.; Manners, I.; Ozin, G. A. *Nature Photon.* **2007**, *1*, 468.
(41) Takeoka, Y.; Watanabe, M. *Adv. Mater.* **2003**, *15*, 199.
(42) Queffelec, J.; Gaynor, S. G.; Matyjaszewski, K. *Macromolecules* **2000**, *33*, 8629.
(43) Tokuda, H.; Tsuzuki, S.; Susan, M. A. B. H.; Hayamizu, K.; Watanabe, M. *J. Phys. Chem. B* **2006**, *110*, 19593.
(44) von Werne, T.; Patten, T. *J. Am. Chem. Soc.* **2001**, *123*, 7497.

weight (M_n) and polydispersity index (M_w/M_n) of the PBnMA and PMMA grafts that were cleaved from the silica cores by HF treatment were characterized using gel permeation chromatography (GPC).

Preparation of Suspensions in IL. The polymer-grafted silica nanoparticles were suspended in THF by ultrasonication, and then the appropriate amount of $[C_2mim][NTf_2]$ was added to the suspension. The suspension was filtered with a 1.0 μm pore-sized filter, and THF was gently removed at room temperature with stirring, followed by complete drying under reduced pressure at 40 °C.

Measurements. GPC was carried out at 40 °C on an LC-10AD liquid chromatography system (Shimadzu) equipped with two columns (TSKgel G4000H and G3000H, Tosoh) and a refractive index detector (RID-10A, Shimadzu). THF was used as the carrier solvent at a flow rate of 1.0 mL min^{-1}. Polystyrene standards were used to calibrate the GPC system. Thermogravimetric analysis (TGA) was conducted from room temperature to 550 °C under a N_2 atmosphere with a heating rate of 10 °C min^{-1} with a TG/TDA6200 (Seiko Instruments Inc.). Turbidity measurements were carried using an UV−vis spectrometer (USB 2000, Ocean optics). Transmittance at 500 nm was monitored with increasing temperature. DLS measurements were performed with a DLS-8000 optical system (Otsuka Electronics Co., Ltd.) equipped with an ALV-5000/60X0 correlator (ALV, Langen) at 633 nm (He−Ne laser) and 488 nm (Ar laser). Experiments were performed at different temperatures (25 °C−110 °C), and the correlation functions were recorded at various scattering angles between 40 and 120 °C. The correlation functions were fitted using an ALV-5000/60X0 correlation system (ALV, Langen). The average hydrodynamic diameter (D_h) and the size distribution function were determined by the fitting cumulant method and CONTIN analysis, respectively.[34] For each temperature, the sample was equilibrated for 30 min prior to the measurements. The reported values of viscosity and refractive index of the IL were used to calculate D_h.[28] Rheological measurements were performed on a rheometer (Physica MCR301, Anton Paar) under dry air conditions at different temperatures. Three different geometries were employed for the measurements: two types of cone-and-plate systems, one with a diameter of 25 mm (cone angle = 2°) and the other with a diameter of 50 mm (1°), as well as a parallel plate system with a diameter of 25 mm, which was used in heating conditions. To erase any previous shear histories and to make the samples establish their equilibrium structures, a steady preshear was applied at a shear rate of 0.1 s^{-1} for 60 s followed by a 120 s rest period before each dynamic rheological measurement. The dynamic measurements were conducted in the linear viscoelastic regime. TEM observation was performed with a JEOL JEM2000FXII operated at 100 kV. The reflection spectra were obtained using an Ocean Optics USB2000 optical-fiber spectrometer.[37]

Results and Discussion

Thermosensitivity of Dilute Suspensions of Polymer-Grafted Silica Nanoparticles. Polymer chains densely grafted on a solid substrate, referred to as polymer brushes, stretch along the direction normal to the substrate because of steric exclusion between neighboring polymer chains. Such polymer brushes can therefore present physical and chemical properties different from corresponding free polymers in solution.[45] Herein, we studied how the extended conformation of PBnMA brushes grafted onto spherical silica particles affects the LCST phase behavior in an IL. The temperature responsive behavior of PBnMA-*g*-NPs was compared with that of the corresponding free PBnMA solution and PMMA-*g*-NPs. A thermally triggered dispersion−aggregation change for PBnMA-*g*-NPs resulting from the solvation−desolvation of PBnMA was also demonstrated in the IL.

Table 1. Characterization of Polymer-Grafted Silica Nanoparticles: Silica Core Diameter, Number-Average Molecular Weight (M_n), Polydispersity Index (M_w/M_n), and Grafting Density (σ)

	silica core diameter (nm)	M_n (kDa)	M_w/M_n	σ (chains/nm^2)
PBnMA-grafted	120	101	1.43	0.29
PMMA-grafted	120	61	1.61	0.20

The surface-initiated ATRP is a representative method to prepare end-grafted polymers with a high grafting density (σ).[46] The σ values (chain nm^{-2}) were calculated from differences of weight loss between bare silica particles and the polymer grafted particles measured by TGA, M_n, and the mass of a single silica particle.[47] Table 1 shows M_n, M_w/M_n, and σ for PBnMA- and PMMA-*g*-NPs used in this study. The σ values for PBnMA- and PMMA-*g*-NPs are 0.29 and 0.20, respectively, and these are similar to the reported σ values of polymer-grafted particles prepared by surface-initiated ATRP.[47,48] Genzer and co-workers reported that mushroom-to-brush change of surface anchored polyacrylamide (PAA, M_w = 17 kDa) occurs at σ of 0.065 chain nm^{-2}.[49] When the size of each monomer unit is taken into consideration, PMMA and PBnMA units should be comparable to or larger than PAA unit, and further the grafted chains have much higher molecular weight than the PAA. The σ values for the grafted PMMA and PBnMA were much higher than the crossover point of the surface-anchored PAA. Thus, it appears certain that both PBnMA and PMMA are densely immobilized on the silica surface so that the grafted polymers behave as a polymer brush. In addition, it should be noted that the polymer chains are tethered to the curved surfaces of the spherical silica in a radial manner, and therefore the outer part of the polymer segments far from the silica core should be more loosely packed than the inner part of the polymer segments, which are close to the core.[50] The grafting chain density is a function of distance from the silica surface. For example, the local density of the outermost part of PBnMA-*g*-NPs can be estimated to be 0.03 chain nm^{-2} at 25 °C, which is roughly 10 times lower than the innermost density (i.e., σ = 0.29 chain nm^{-2}).

Figure 1a shows the temperature dependence of turbidity for a 3 wt % free PBnMA (M_w = 70 kDa, obtained from Aldrich) solution in $[C_2mim][NTf_2]$. The solution is transparent below 105 °C and suddenly becomes cloudy at 106 °C. This transition occurs in a very narrow temperature range (< 2 °C). This discrete transition was also microscopically revealed by DLS measurements. Free PBnMA chains were suddenly desolvated to form large aggregates at the phase separation temperature, while the hydrodynamic size of PBnMA did not change with increasing temperature before the phase separation.[28] Figure 1b shows the temperature dependence of the hydrodynamic diameter (D_h) of PBnMA- and PMMA-*g*-NPs in $[C_2mim][NTf_2]$. For PMMA-*g*-NPs whose PMMA chains are soluble in $[C_2mim][NTf_2]$ irrespective of temperature over a wide range (30−300 °C),[28] there is little change in D_h in the temperature range from 25 to 110 °C. On the contrary, D_h for PBnMA-*g*-NPs monotonically decreases from

(45) Brittain, W. J.; Minko, S. *J. Polym. Sci., Part A: Polym. Chem.* **2007**, *45*, 3505.

(46) Barbey, R.; Lavanant, L.; Paripovic, D.; Schüwer, N.; Sugnaux, C.; Stefano Tugulu, S.; Klok, H.-A. *Chem. Rev.* **2009**, *109*, 5437.

(47) Li, D.; Jones, G. L.; Dunlap, J. R.; Hua, F.; Zhao, B. *Langmuir* **2006**, *22*, 3344.

(48) Li, D.; Sheng, X.; Zhao, B. *J. Am. Chem. Soc.* **2005**, *127*, 6248.

(49) Wu, T.; Efimenko, K.; Genzer, J. *J. Am. Chem. Soc.* **2002**, *124*, 9394.

(50) Savin, D. A.; Pyun, J.; Patterson, G. D.; Kowalewski, T.; Matyjaszewski, K. *J. Polym. Sci., Part B: Polym. Phys.* **2002**, *40*, 2667.

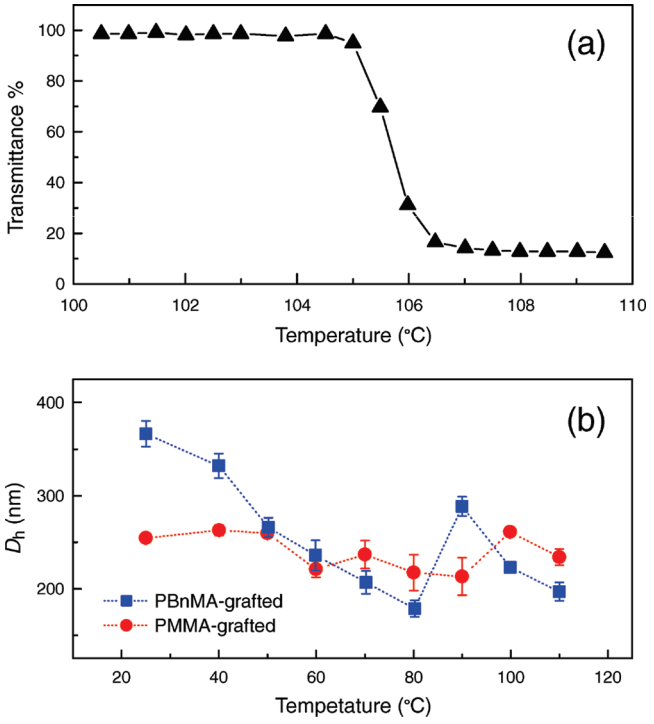

Figure 1. (a) Temperature dependence of transmittance at 500 nm for 3 wt % free PBnMA (M_w = 70 kDa)/[C_2mim][NTf_2] solution and (b) temperature dependence of hydrodynamic diameters (D_h) for PBnMA-grafted (square, 0.0073 wt %) and PMMA-grafted (circle, 0.023 wt %) silica nanoparticles in [C_2mim][NTf_2].

375 nm at 25 °C to 179 nm at 80 °C and suddenly increases at 90 °C followed by decreasing again above 100 °C.

In comparison with the transition of free PBnMA chains as shown in Figure 1a, there are two major differences in the temperature responsive properties of PBnMA-*g*-NPs in [C_2mim][NTf_2]: (i) the grafted PBnMA collapsed at much lower temperature than T_c for free PBnMA, and (ii) the transition of the grafted PBnMA chains is much broader than that of free PBnMA. These features qualitatively coincide with the transition behaviors of thermosensitive polymer brushes immobilized on gold nanoparticles,[51] latex particles,[52,53] dendrimers,[54] and silica nanoparticles[47,55] compared to the corresponding free polymer aqueous solutions. The lowered phase transition temperature may be attributed to a higher local concentration of PBnMA grafted onto silica nanoparticles because T_c of PBnMA decreases with increasing polymer concentrations (see Supporting Information, Figure S1). Furthermore, broadening of the transition is likely due to both the brushlike conformation of PBnMA, which leads to strong interchain interactions,[56] and the local concentration distribution, which depends on the inner and outer part of the grafted PBnMA in a radial manner, as described above. The local concentration of the PBnMA segments in the inner region is higher than that in the outer region. Hence, the inner segments collapse at lower temperatures than the outer segments. In fact, below 90 °C, the particle remains stable due to steric repulsive forces in the outer region of grafted PBnMA. However, an increased D_h is observed

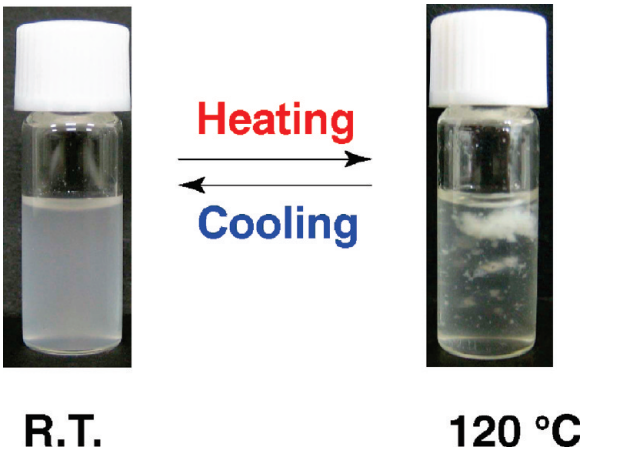

Figure 2. Optical images of 1 wt % PBnMA-grafted silica colloidal suspension in [C_2mim][NTf_2] at room temperature (left) and 120 °C (right).

at 90 °C, indicating flocculation of the PBnMA-*g*-NPs caused by desolvation of the outermost region. When the outermost PBnMA changes to solvophobic, the interaction between the particles becomes attractive and the particles no longer remain stable in the IL. Above 100 °C, we observe a further decrease in D_h with the simultaneous observation that the scattering intensity of DLS significantly decreases. This suggests that the large aggregates are segregated from the suspension system and are not detected. Only the desolvated particles that are not flocculating are detected by the DLS measurement. We conclude that the transition from suspension to aggregation occurred at 90 °C. At 120 °C, PBnMA-*g*-NPs were completely phase-separated, as shown in Figure 2. Because of the lower density of PBnMA-*g*-NPs than [C_2mim][NTf_2], the aggregates can be seen in the upper portion of the sample tube. These aggregated PBnMA-*g*-NPs can be resuspended with cooling below 80 °C and shaking of the sample tube.

In summary, dilute suspensions of PBnMA-*g*-NPs in [C_2mim][NTf_2], PBnMA-*g*-NPs undergo the LCST transition at a lower temperature, within a broader temperature range, compared to the LCST behavior of the free PBnMA solution. The desolvation of PBnMA densely tethered to spherical silica starts from the inner region and spreads to the outer region upon heating. The aggregation of the particles occurs as the outermost PBnMA became solvophobic at 90 °C. This unique transition of grafted PBnMA plays a role in the properties of the soft glassy colloidal array (vide infra).

Soft Glassy Colloidal Arrays: Optical and Rheological Properties. In previous work, we reported that highly concentrated suspensions of PMMA-*g*-NPs in [C_2mim][NTf_2] formed soft glassy colloidal arrays (SGCAs) and exhibited a soft-solid character and homogeneous, nonbrilliant, and angle-independent structural colors.[37,38] Figure 3 indicates the appearances of the colloidal suspensions of polymer-grafted silica nanoparticles in the IL with different particle concentrations. The dilute suspensions (samples B and C in Figure 3) are fluid, while the dense suspensions (samples D−G) are solidified and exhibit different colors depending on the particle concentration. PBnMA-*g*-NPs can, of course, form a SGCA (sample D in Figure 3) above 14.2 wt % at room temperature. Such solidification of the concentrated suspension can be understood as a colloidal glass transition.[38,57] It is known that hard-sphere repulsive particles can form colloidal

(51) Shan, J.; Chen, J.; Nuopponen, M.; Tenhu, H. *Langmuir* **2004**, *20*, 4671.
(52) Zhu, P. W.; Napper, D. H. *J. Phys. Chem. B* **1997**, *101*, 3155.
(53) Kizhakkedathu, J. N.; Norris-Jones, R.; Brooks, D. E. *Macromolecules* **2004**, *37*, 734.
(54) Luo, S.; Xu, J.; Zhu, Z.; Wu, C.; Liu, S. *J. Phys. Chem. B* **2006**, *110*, 9132.
(55) Wu, T.; Zhang, Y.; Wang, X.; Liu, S. *Chem. Mater.* **2008**, *20*, 101.
(56) Balamurugan, S.; Mendez, S.; Balamurugan, S. S.; O'Brien, M. J., II; López, G. P. *Langmuir* **2003**, *19*, 2545.
(57) Pusey, P. N.; van Megen, W. *Nature* **1986**, *320*, 340.

Figure 3. Appearance of PMMA- and PBnMA-grafted silica colloidal suspensions in [C_2mim][NTf_2]. Concentrations: A, pure [C_2mim][NTf_2]; B, PMMA-grafted (1.0 wt %); C, PMMA-grafted (3.0 wt %); D, PBnMA-grafted (14.2 wt %); E, PMMA-grafted (18.0 wt %); F, PMMA-grafted (25.0 wt %); G, PMMA-grafted (35.0 wt %).

glass at high particle concentrations, where the particles are trapped within cages formed by the nearest neighbors, showing solidlike properties due to the "cage effect" for the crowding of the particles.[58,59] As for the unique optical properties, the colloidal systems do not contain any chromophores capable of absorbing visible light. The colors were determined to be the consequence of the structural colors caused by the scattering of coherent light from the "short-range ordered" glassy colloidal array, which was revealed by 2D Fourier analysis of TEM images for SGCA and the predicted reflection spectra from the 2D Fourier power spectra.[37,38] The structural colors of the SGCAs were also homogeneous, nonbrilliant, and angle-independent (Supporting Information, Figure S2). These optical properties are consistent with the reported results of a photonic amorphous material showing short-range order, calculated by the multiple-scattering method.[60] Recently, Takeoka et al. explained the unique structural colors of amorphous colloidal arrays using the "tight bonding model", as was applied to the characterization of the electronic band gap of semiconductors.[61]

To characterize the viscoelastic behavior of the SGCAs in the IL, we conducted low-amplitude oscillatory shear measurements. The results of the dynamic rheological properties for SGCAs of PBnMA-*g*-NPs at 25 °C are shown in Figure 4. For all of the samples examined, the storage modulus (G') is significantly larger than the loss modulus (G'') and is almost independent of frequency over the entire frequency range from 0.1 to 100 rad s^{-1}, indicating that the systems give solidlike responses. The plateau G' increases with increasing particle concentration and shows power-law dependence on the particle concentration (Figure 4, inset). Unlike hard-sphere particles, the polymer-grafted particles are deformable and/or interpenetrable because of the loose outer-grafting polymer layer. Therefore, the overpacking of the particle concentration can occur[38] even above the random closest packing ratio (0.64) for a hard-sphere system.[62] This particle softness results in the increased density of the particles even in the glassy state of SGCAs, which enhances the elasticity of the SGCAs.[38] Similar results are reported in highly packed microgel suspension

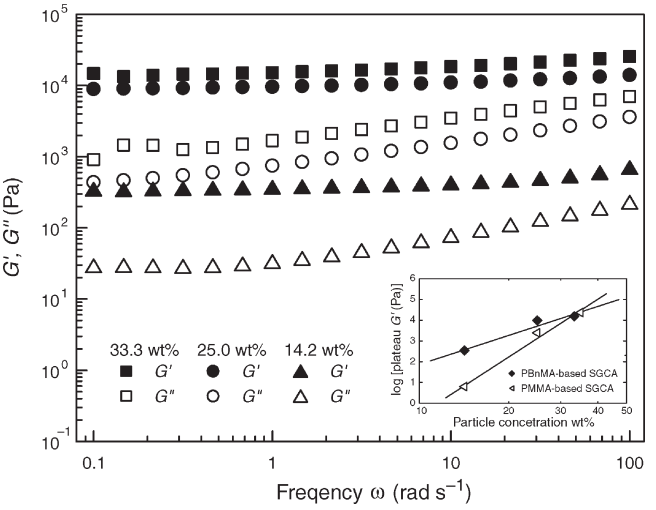

Figure 4. Elastic (G') and loss (G'') moduli as a function of frequency for SGCAs of PBnMA-*g*-NPs in [C_2mim][NTf_2] with different particle concentrations at 25 °C. The inset shows logarithmic plots of plateau G' as a function of the particle concentration in the SGCAs. The solid lines represent the results of power-law fitting.

systems, where the plateau G' showed power-law dependence on the volume fraction proportional to particle concentration.[63]

Temperature-Induced Colloidal Glass to Gel Transition. Here we show temperature-responsive properties of the SGCAs consisting of PBnMA-*g*-NPs. Figure 5 represents the temperature dependence of G' and G'' for SGCAs composed of PMMA- and PBnMA-*g*-NPs. The measurements were taken at the strain γ = 1%, frequency ω = 1 rad s^{-1}, and the heating rate = 0.5 °C min^{-1}. As expected from the thermosensitivity of the dilute suspensions shown in Figure 1b, there are no significant changes in G' and G'' in SGCA composed of PMMA-*g*-NPs (Figure 5a); the viscoelastic properties of PMMA-based SGCA are irresponsive to temperature. In contrast, PBnMA-based SGCA displays an interesting viscoelastic behavior in response to temperature (Figure 5b). Both G' and G'' first decrease with rising temperature up to 95 °C and then increase at higher temperatures. Such a V-shaped rheological response is interpreted in relation to the thermosensitivity of PBnMA-*g*-NPs, as discussed for diluted suspensions in

(58) Mason, T. G.; Weitz, D. A. *Phys. Rev. Lett.* **1995**, *75*, 2770.
(59) Stokes, J. R.; Frith, W. J. *Soft Matter* **2008**, *4*, 1133.
(60) Jin, C.; Meng, X.; Cheng, B.; Li, Z.; Zhang, D. *Phys. Rev. B* **2001**, *63*, 195107.
(61) Takeoka, Y.; Honda, M.; Seki, T.; Ishii, M.; Nakamura, H. *ACS Appl. Mater. Interfaces* **2009**, *1*, 982.
(62) Scott, G. D. *Nature* **1960**, *188*, 908.
(63) Senff, H.; Richtering, W. *Colloid Polym. Sci.* **2000**, *278*, 830.

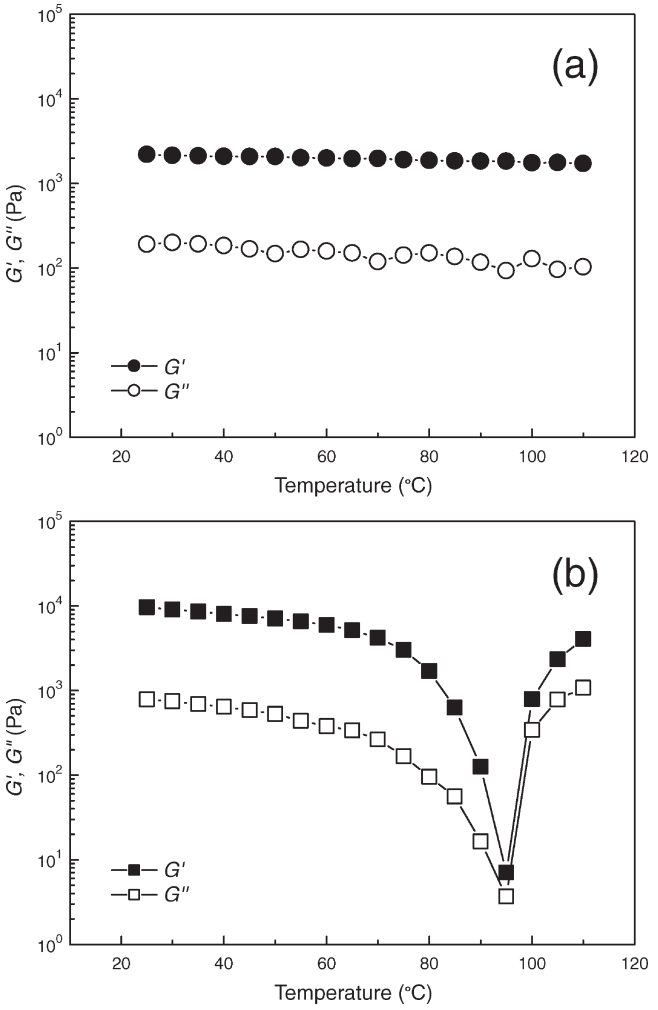

Figure 5. Temperature dependence of storage modulus G' (filled) and loss modulus G'' (open) for 25.0 wt % (a) PMMA-based and (b) PBnMA-based SGCAs in $[C_2mim][NTf_2]$. The measurements were carried out at strain $\gamma = 1\%$, frequency $\omega = 1$ rad s^{-1}, and heating rate = 0.5 °C min^{-1}.

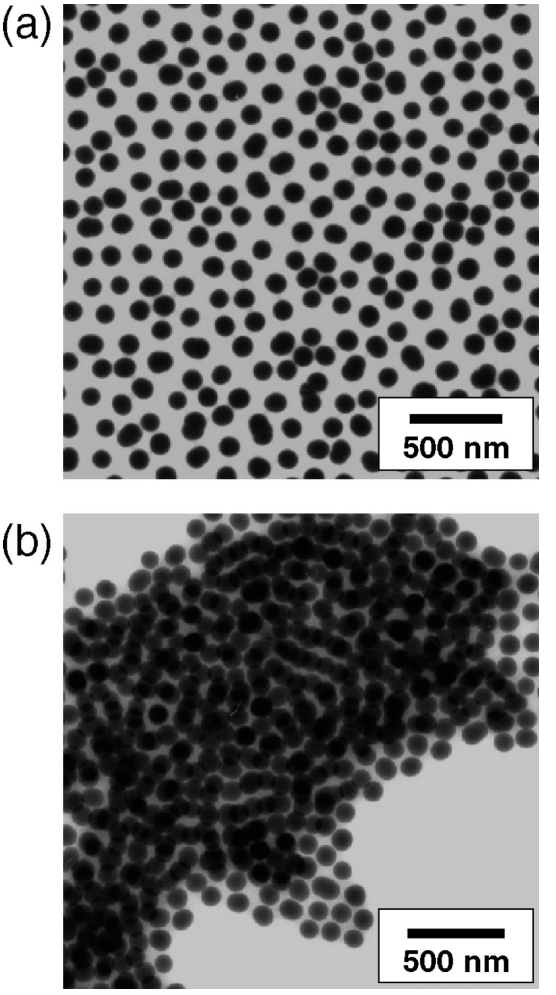

Figure 6. In-situ TEM images of 25.0 wt % PBnMA-based SGCA in $[C_2mim][NTf_2]$ (a) before and (b) after heating at 100 °C.

the previous section. The first decrease in the moduli is governed by the lowering of the particle volume fraction, which arises from deswelling of the inner layer of the grafting PBnMA. At 95 °C, G' is significantly lowered and is comparable to G'', suggesting that the particles are relatively free from the cages of the neighboring particles and the system shows fluidity. Above 95 °C, the difference between G' and G'' becomes larger again. Since the outermost PBnMA should be desolvated and PBnMA-*g*-NPs are no longer colloidally stable at this temperature range, an interconnected particulate network, or gel, is formed by the flocculated particles, and therefore a solidlike response ($G' \gg G''$) is observed. Recently, Narayanan et al. a reported similar V-shaped rheological response as a function of temperature by employing dense suspensions of silica particles coated with stearyl alcohol in *n*-dodecane.[64] However, the stearyl-substituted silica particles exhibited temperature sensitivity opposite to that of PBnMA-*g*-NPs, where the interparticle interaction of the stearyl-substituted silica particles was attractive at lower temperatures and repulsive at higher temperatures.

In order to confirm the aggregated structure of PBnMA-*g*-NPs in the IL, TEM images were taken in the presence of the IL as reported in our previous work.[34,35,37] Even under a high-vacuum condition and electron beam irradiation, ILs can be observed by a scanning electron microscope and a transmission electron microscope (TEM) without evaporation and without the accumulation of electronic charges. Therefore, by direct TEM observations using ILs as dispersion media, we can evaluate visually the dispersibility and microstructure of colloidal materials in ILs. Figure 6 shows the TEM images of 25% PBnMA-based SGCA before and after heating at 120 °C. Because of the slow kinetics of redissolution for the desolvated PBnMA in $[C_2mim][NTf_2]$,[29] the aggregated structure can be maintained during TEM observation by quenching the sample. Most of the silica core particles before heating were separated from each other by PBnMA chains, while the particles adhered with each other and formed large aggregates after heating. As a result, these observations prove that the solidlike rheological response at temperatures above 95 °C reflected the formation of a gel due to the flocculation of PBnMA-*g*-NPs into particulate networks.

There are two categories of solidlike amorphous soft materials consisting of colloidal particles: colloidal glass formed by random packing of a high volume fraction of particles or colloidal gel in which a low volume fraction of colloidal particulate networks percolate throughout the entire volume of suspension medium.[56] According to this classification, we recognize this temperature-induced, V-shaped viscoelastic behavior as a colloidal glass-to-gel transition. Namely, PBnMA-based SGCA (colloidal glass) can be

(64) Sztucki, M.; Narayanan, T.; Belina, G.; Moussaïd, A.; Pignon, F.; Hoekstra, H. *Phys. Rev. E* **2006**, *74*, 051504.

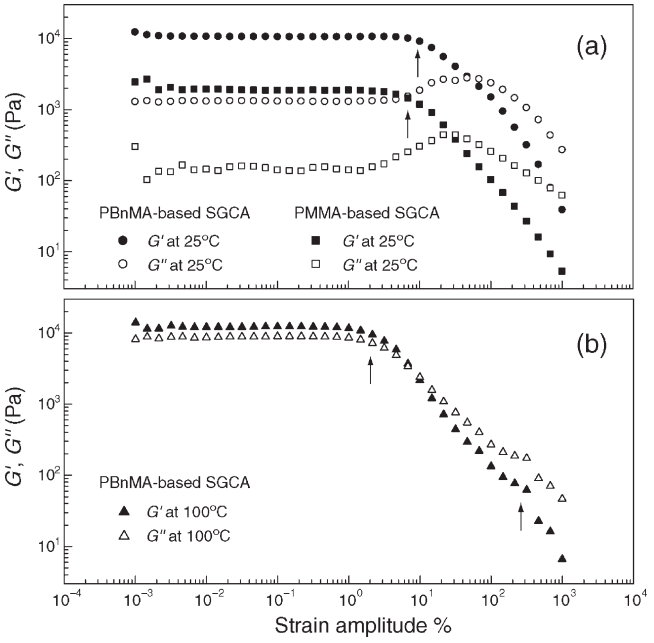

Figure 7. Dynamic strain sweep for 25 wt % (a) PMMA- and PBnMA-based SGCAs at 25 °C and (b) PBnMA-based SGCAs at 100 °C in [C_2mim][NTf_2]. The frequency was held constant at 6.28 rad s^{-1}. The arrows indicate the yielding strains.

transformed into a colloidal gel in which the outermost PBnMA shrinks and the interparticle attractive force is dominant. Furthermore, we found that lower particle concentrations of the suspension, which show liquidlike, viscous responses at 25 °C, can also behave as a soft solid at temperatures above 120 °C due to the formation of the particulate network (i.e., liquid-to-gel transition, Supporting Information, Figure S3).

The difference between colloidal glass and colloidal gel has been characterized by investigating the yielding behaviors in strain sweep measurements. Poon and co-workers revealed that hard-sphere repulsive glass and colloidal gel exhibited single- and two-step yielding, respectively.[65] Figure 7 shows the elastic G' and viscous G'' moduli as functions of the strain amplitude for PBnMA-based SGCAs at 25 and 100 °C and PMMA-based SGCAs at 25 °C. While G' is larger than G'' within the region of linear viscoelasticity, the transition from a solidlike ($G' > G''$) to a liquidlike ($G' < G''$) behavior is detected for the high strain amplitudes in all of the samples. Single-step yielding is observed in PMMA- and PBnMA-based SGCAs at 25 °C, when the suspension is categorized as a colloidal glass (Figure 7a). The yielding starts at strain (γ) ~ 7% for PMMA-based SGCA and $\gamma \sim 10\%$ for PBnMA-based SGCA. The single yielding is likely due to distortion of the cage of nearest neighbors around each particle. At 100 °C, however, PBnMA-based SGCA forming a colloidal gel shows well-defined two-step yielding at $\gamma \sim 2\%$ and $\gamma \sim 300\%$, as indicated by the arrows in Figure 7b. These observations were in agreement with the previous study.[65] Indeed, the two-step yielding behavior was also found in our previous colloidal gel composed of unmodified silica nanoparticles in an IL.[35] For the two-step yielding, the first and second yield strain may be assigned as the strain required to barely disrupt the interparticle bonds that form the network and the strain needed to cause the sample to flow, respectively. Thus, the transition from a low-temperature

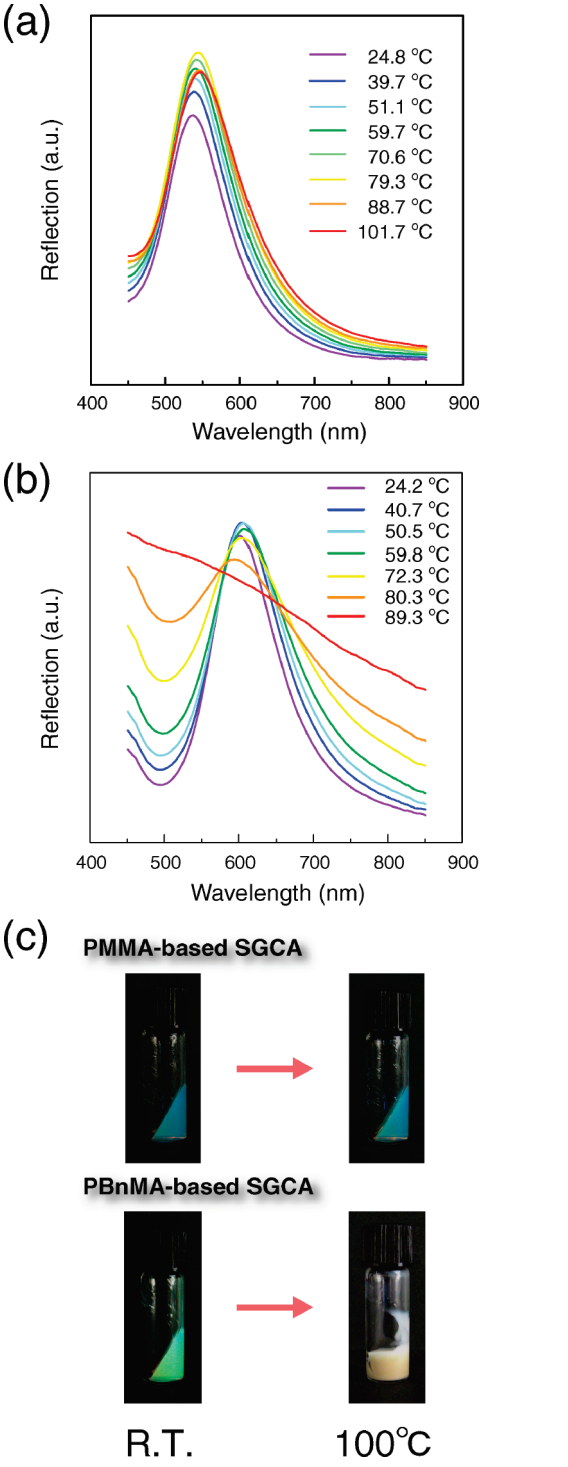

Figure 8. Reflection spectra of 25 wt % (a) PMMA- and (b) PBnMA-based SGCA in [C_2mim][NTf_2] at different temperatures. (c) Structural color changes in SGCAs before and after heating at 100 °C.

colloidal glass to a high-temperature colloidal gel of PBnMA-based SGCA is also verified by the corresponding yielding behavior.

With regard to the glass-to-gel transition temperature in PBnMA-based SGCA (Figure 5), the minimum of the moduli is found at 95 °C, which is slightly higher than the aggregation temperature (90 °C) of PBnMA-*g*-NPs in the dilute suspension. Since the thermosensitive rheology was studied by temperature sweep measurements, this observation may be linked to the colloidal dynamics that form interconnecting networks after the particles

(65) Pham, K. N.; Petekidis, G.; Vlassopoulos, D.; Egelhaaf, S. U.; Pusey, P. N.; Poon, W. C. K. *Europhys. Lett.* **2006**, *75*, 624.

shrink at the aggregation temperature. Indeed, the transition temperature showing minima of the moduli depends on particle concentration (Supporting Information, Figure S4). Lower transition temperatures are observed for higher concentrations of SGCA, where the interparticle distance is shorter, and thereby collision occurs more frequently in the absence of interparticle repulsion.

Figure 8 shows the temperature dependence of reflection spectra and photographs for the PMMA- and PBnMA-based SGCAs. At room temperature, both SGCAs exhibited reflection peaks corresponding to the observed colors. The maximum wavelengths of the reflection peaks are 540 nm for PMMA-based SGCA and 600 nm for PBnMA-based SGCA. Since these reflection peaks are derived from coherent scattering from the short-range ordered structure in SGCAs, the higher M_n of the grafting polymer (i.e., larger interparticle distance) for PBnMA-*g*-NP resulted in a larger maximum wavelength of the reflection peak as compared to PMMA-SGCA. Although no remarkable temperature-dependent change in peak position is observed for PMMA-based SGCA, the full width at half-maximum (fwhm) of the reflection peak slightly increased with increasing temperature (Figure 8a). This may be responsible for the changes in the refractive indices of SGCA with temperature and/or the Debye−Waller effect due to the thermal motion of the particles.[66] Nevertheless, the structural color remains unchanged even after heating, as shown in Figure 8c. For PBnMA-based SGCA, the base lines of the reflection peaks significantly increase and the peak intensity weakens upon heating (Figure 8b). In comparison to PMMA-based SGCA, PBnMA-based SGCA presented a drastic increase in fwhm with an increase in temperature. In this case, the Debye−Waller effect appears to be increased by a decrease in the particle volume fraction, which provides available space for more active thermal fluctuation of the particles. The more enhanced intensity in the shorter wavelength range at higher temperatures is indicative of incoherent scatterings such as Rayleigh and Mie scatterings, where the scattering intensity decreases with wavelength.[67] The reflection peak is no longer detected at 89.3 °C. After heating at 100 °C, the solution becomes opaque (Figure 8c). This temperature dependency of the optical properties is in agreement with the thermosensitivity of PBnMA-*g*-NP in the IL. With the glass-to-gel transition of PBnMA-based SGCA, the short-range ordered structure is transformed into a completely disordered structure (Figure 6). Therefore, the incoherent scattering arising from aggregated PBnMA chains and the particles plays a predominant role in the optical properties of the colloidal gel of the heated SGCA, where most of the incident light is randomly scattered. Moreover, we confirmed that this color change is reversible although it takes a relatively long time (~10 days at the least) due to the slow dynamics of PBnMA redissolution. Such a slow responsive rate on cooling can be improved by optimizing the chemical structures of the grafting polymers and the ILs.[29]

(66) Rundquist, P. A.; Kesavamoorthy, R.; Jagannathan, S.; Asher, S. A. *J. Chem. Phys.* **1991**, *95*, 1249.
(67) Gao, J.; Hu, Z. *Langmuir* **2002**, *18*, 1360.

Conclusion

We prepared polymer-grafted silica nanoparticles, PMMA-*g*-NP and PBnMA-*g*-NP, by means of surface-initiated ATRP and investigated their thermosensitive properties in an IL ranging from diluted to concentrated solutions. In the dilute suspensions, PBnMA-*g*-NPs underwent LCST phase separation at lower temperatures and over a broader temperature range in comparison to the free PBnMA solution, while PMMA-*g*-NPs were almost irresponsive to temperature. This unique thermosensitive behavior was attributed to the fact that the PBnMA chains were immobilized on the spherical silica surface with a high graft density. The lower transition temperature may have been a result of the high local concentration, whereas the broader temperature range was attributed to both the brushlike conformation and local concentration distribution of the PBnMA chains in a radial manner. We concluded that the inner PBnMA segments collapsed at a lower temperature than the outer ones. The concentrated suspensions formed soft glassy colloidal arrays (SGCAs) exhibiting a soft-solid behavior and various structural colors. In analogy to the dilute system, no remarkable change was observed in the PMMA-based SGCAs with temperature. The PBnMA-based SGCAs exhibited a V-shaped rheological response and structural color changes in response to temperature. These thermosensitive properties were derived from the colloidal glass-to-gel transition synchronized with the phase transition of PBnMA-NPs in the IL.

With unique rheological and optical properties as well as the properties derived from the IL itself, the thermosensitive SGCAs may be useful in developing new materials for a wide range of applications such as electrochemical devices and color displays with wide viewing angles.

Acknowledgment. This work was supported by a Grant-in-Aid for Scientific Research from the Ministry of Education, Culture, Sports, Science and Technology (MEXT), Japan (#452-17073009 and #B-20350104). K.U. acknowledges financial support provided by JSPS.

Supporting Information Available: Concentration dependence of T_c for the free PBnMA solutions, transmission spectra for angle-independent structural color, rheological data on the liquid-to-gel transition, and the temperature sweep rheological data with different particle concentrations. This material is available free of charge via the Internet at http://pubs.acs.org.